



Elemental profiles of swine tissues as descriptors for the traceability of value-added Italian heavy pig production chains

Maria Olga Varrà^a, Lenka Husáková^b, Emanuela Zanardi^{a,*}, Giovanni Loris Alborali^c, Jan Patočka^b, Adriana Ianieri^a, Sergio Ghidini^a

^a Department of Food and Drug, University of Parma, Strada del Taglio, 10, 43126 Parma, Italy

^b Department of Analytical Chemistry, Faculty of Chemical Technology, University of Pardubice, Studentska 573 HB/D, Pardubice CZ-532 10, Czech Republic

^c Istituto Zooprofilattico Sperimentale della Lombardia e dell'Emilia-Romagna, Via A. Bianchi 9, 25124 Brescia, Italy

ARTICLE INFO

Keywords:

Meat composition
Minerals
Labelling
Inductively coupled plasma mass spectrometry
Chemometrics

ABSTRACT

The increasing demand for reliable traceability tools in the meat supply chain has prompted the exploration of innovative approaches that meet stringent quality standards. In this work, 57 elements were quantified by inductively coupled plasma mass spectrometry and direct mercury analysis in 80 muscle and 80 liver samples of Italian heavy pigs to investigate the potential of new tools based on multi-elemental profiles in supporting value-added meat supply chains. Samples from three groups of animals belonging to the protected designation of origin (PDO) Parma Ham circuit (conventionally raised; raised with genetically modified organism (GMO)-free feeds; raised with GMO-free feeds plus the supplementation of omega-3 polyunsaturated fatty acids (n-3 PUFA)) and a fourth group of samples from animals not compliant with the PDO Parma Ham production process were analyzed. Hierarchical cluster analysis allowed for the identification of three macro-clusters of liver or muscle samples, highlighting some inhomogeneities among the target groups. Following SIMCA analysis, better classification models were obtained by using liver elemental profiles (95% correct classification rate), with the highest classification accuracy observed for GMO-free livers (100%). The elements contributing the most to the separation of livers by class membership were La, Ce, and Pb for conventional, Li, Cr, Fe, As, and Sr for GMO-free + n-3 PUFA, and Lu for non-PDO samples. Given these findings, the analysis of the elemental profiles of pig tissues can be regarded as a promising method to confirm the declared pig meat label attributes, deter potential complex fraud, and support meat traceability systems.

1. Introduction

The heavy pig production chain represents a very important source of typical and high-quality processed meat products in Spain, Italy, France, Germany, Poland, and Greece. Indeed, due to the heavy weight and the adequate amount of subcutaneous adipose tissue, pork cuts obtained from carcasses of heavy pigs are particularly suitable for salting and seasoning and allow for the production of Protected Denomination of Origin (PDO) products, including Parma Ham (Halagarda, Kędzior, & Pyrzyńska, 2017; Halagarda & Wójciak, 2022; Resano et al., 2011). In Italy alone, approximately 10 million heavy pigs are

annually slaughtered, corresponding to 95% of the total slaughtered pig population (Italian National Institute of Statistics, 2023). From these, 90,000 tons of PDO Parma Ham are produced, which represent 45% of the overall quantity of Italian meat products certified by quality marks (Italian Ministry of Agriculture, Food and Forestry, 2020). Parma Ham is obtained from the dry curing of fresh hind legs of heavy pigs of specific breeds, raised in a limited area of northern Italy, and slaughtered at a minimum age of 9 months and a live weight of 160 kg plus 15% or less 10% after long finishing phases (Italian Ministry of Agriculture, Food Sovereignty and Forests, 2022). Heavy pigs dedicated to PDO Parma Ham production must also be fed with well-defined and rationed diets in

Abbreviations: ANOVA, analysis of variance; CRM, certified reference material; GMO, genetically modified organism; HCA, hierarchical cluster analysis; ISTD, internal standard; ICP-MS, inductively coupled plasma mass spectrometry; MANOVA, multivariate analysis of variance; MLOD, method limit of detection; MLOQ, method limit of quantification; MP, modeling power; NCA, neighborhood component analysis; PDO, protected designation of origin; PUFAs, polyunsaturated fatty acids; REEs, rare earth elements; SIMCA, soft independent modeling of class analogy.

* Corresponding author.

E-mail address: emanuela.zanardi@unipr.it (E. Zanardi).

<https://doi.org/10.1016/j.meatsci.2023.109285>

Received 8 March 2023; Received in revised form 14 July 2023; Accepted 16 July 2023

Available online 17 July 2023

0309-1740/© 2023 The Authors. Published by Elsevier Ltd. This is an open access article under the CC BY-NC-ND license (<http://creativecommons.org/licenses/by-nc-nd/4.0/>).

both the weaning and fattening stages (European Commission, 2013a). Within the PDO Parma Ham circuit, premium-differentiated supply chains are present. These supply chains, mainly designed to meet the heterogeneity of consumers asking for healthier and more sustainable products, offer not only PDO hams but also a wide variety of other fresh or processed meat products. Among these, the so-called “negatively labelled” products obtained from animals that were fed since birth without the use of genetically modified crops, feedstuffs, and ingredients (genetically modified organism-(GMO)-free) can be increasingly found in the marketplace. As a result of a great promotion by the largest Italian food retailers, also pig meat products claiming through the label the presence of n-3 polyunsaturated fatty acids (n-3 PUFA) are becoming more frequent. This label ensures the inclusion of n-3 PUFA-enriched-feedstuffs in animal diets and, by consequence, a higher amount of these compounds in the final meat products (Bartkovský et al., 2022; Dugan et al., 2015).

Both GMO-free and n-3 PUFA-enriched meat supply chains are certified by voluntary schemes issued by third-party certifiers. These schemes ensure that the quality attributes claimed on the labels are backed by compliance with specific requisites imposed on the processors (European Commission, 2013b; Kemper, Popp, Nayga, & Kerr, 2018). Nevertheless, considering that these top-quality certified meat products are considerably more expensive, the potential fraudulent substitution with lower quality/priced ones is a very important and topical issue to be addressed.

It is well known that breeding types and the dietary background can influence not only the organic but also the inorganic composition of the animal tissues (Song et al., 2021; Zhao, Wang, & Yang, 2016). These factors have consequently an important impact on the quality and attributes of the raw meat, which translate into implications for the overall quality of the final processed product (Lebret & Čandek-Potokar, 2022).

Many studies demonstrated that frequency, type, and source of feeding are a major determinant of the inorganic elemental composition of pig livestock, especially when animals are raised in low-polluted areas (Blanco-Penedo et al., 2010; Jiang, Tang, Xue, Lin, & Xiong, 2017; López-Alonso, García-Vaquero, Benedito, Castillo, & Miranda, 2012; Oliveira, Alewijn, Boerrigter-Eenling, & van Ruth, 2015; Parinet et al., 2018; Wójciak et al., 2021; Zhao et al., 2020, 2016). Indeed, as monogastric animals, pigs easily transfer macro- and micro-components ingested through the diet into their tissues, whose composition may therefore reflect that of the feed (Reig, Aristoy, & Toldrá, 2013). Within this context, the specific environmental and processing conditions in which Italian heavy pigs destined for PDO Parma Ham are raised directly influence the inorganic chemical composition of the resulting meat products (Bosi & Russo, 2004). Furthermore, previous research indicates that genetically modified crops exhibit distinct characteristics in their absorption and metabolism of elements from the soil (Hrbek et al., 2017; Liu, Feng, Liu, Peng, & He, 2019), implying that both GMO and GMO-free feed ingredients may have specific elemental profiles that can be passed on to pig tissues. As Italy prohibits the cultivation of genetically modified crops (European Parliament and Council of the European Union, 2015; Legislative Decree of the Italian Republic President 227/2016, 2016), they are imported for use in conventional swine supply chains, while the GMO-free supply chains procure crops locally. This may suggest that feed ingredients grown in Italy may exhibit a distinctive elemental signature that can be transferred to pig tissues.

The number of studies dealing with the investigation of the elemental composition of pig tissues and related meat products is limited to the assessment of the risk associated with the presence of toxic metals (Amici, Danieli, Russo, Primi, & Ronchi, 2012; Barone et al., 2021; Ghidini et al., 2022; Halagarda & Wójciak, 2022; López-Alonso et al., 2007) or the verification of mandatory label information such as species (Bilge, Velioglu, Sezer, Eseller, & Boyaci, 2016) and geographic origin (Kim et al., 2017; Park et al., 2018; Qi et al., 2021; Zhao et al., 2020). Only a few research studies have exploited the potential of multi-elemental analysis to authenticate pig meat standing out for superior

quality parameters, such as the extensive or organic method of production (López-Alonso et al., 2012; Nikolic et al., 2017; Oliveira et al., 2015; Parinet et al., 2018; Zhao et al., 2016), the feeding regime (Chalabis-Mazurek et al., 2021; Jerez-Timaure, Sanchez-Hildago, Pulido, & Mendoza, 2021), or certain animal welfare standards (Song et al., 2021). Therefore, collecting data on the occurrence and concentration of macro-, micro-, trace, and ultra-trace elements in pig meat from value-added supply chains is of utmost importance for both authentication and traceability purposes. Indeed, by analyzing these multi-element signatures, reliable markers can be identified to authenticate the origin, production practices, and compliance with safety regulations ensuring that consumers receive genuine and safe products while preventing fraud in the industry. Additionally, comprehensive data on the occurrence and concentration of elements in pig meat products along the supply chain enable the establishment of a transparent and accountable traceability system, facilitating efficient recalls, quality control measures, and enabling prompt responses to potential food safety concerns.

For the first time, the present research explored the inorganic chemical profile of Italian heavy pigs destined to the production of high-value certified meat products via inductively coupled plasma mass spectrometry (ICP-MS) and a mercury analyzer. Overall, 57 elements were quantified in raw muscle and liver tissues of animals from conventional, GMO-free, GMO-free + n-3 PUFA PDO Parma Ham supply chains and investigated through chemometric tools. The multi-elemental profiles obtained from the analysis of raw muscle and liver tissues present considerable potential for developing reliable universal discriminant models for Italian heavy pigs, which can be used to verify the authenticity of raw meat before its transformation into different high-quality meat products. This approach offers the advantage of using more accessible and cost-effective samples, thereby eliminating the need for sampling expensive meat cuts in practical applications.

2. Materials and methods

2.1. Animal selection

Crossbred pigs in line with the PDO Parma Ham Consortium requirements were raised in intensive indoor farms in northern Italy dedicated to the breeding of heavy pigs. Specifically, 60 pigs (at least 9 months aged and weighting 160 kg \pm 10%) raised in 12 different farms (5 animals per farm, randomly selected from individual batches of 135 animals each) and producing pigs for 3 PDO Parma Ham supply chains (4 farms per supply chain) were considered, namely: i) 20 conventionally reared pigs (receiving a standard diet); ii) 20 pigs reared with GMO-free feed formulations; iii) 20 pigs reared with GMO-free feed formulations and receiving also supplementation with n-3 PUFA through extruded linseed during the last three months of fattening phase. The feed provided to animals in each pig farm under consideration was prepared by including exclusively authorized raw materials in accordance with the specific maximum quantities specified in the product specification (European Commission, 2013a).

For comparison purposes with the other 3 groups, an additional pig group consisting of 20 heavy pigs from 4 different farms (5 animals per farm) was considered. These animals were raised without following the specific PDO Consortium requirements for breeding and feeding. Detailed specifications of the sampling plan are reported in Table 1.

2.2. Sample collection and preparation

The collection of samples was performed within two months in an industrial slaughterhouse in northern Italy (Emilia-Romagna region), where pigs were slaughtered according to regular abattoir procedures. Immediately after stunning and exsanguination, the diaphragm muscle (50–100 g) and the right lateral lobe of the liver (400–500 g) were excised from each animal. A total of 80 muscle and 80 liver samples were thus collected. Each sample was individually packed in low-density

Table 1

Animal selection based on the certified supply chain the meat products were destined to.

Group ID	Farm	PDO certification	Supply chain	N. animals
Conventional	1	YES	GMO	5
	2	YES	GMO	5
	3	YES	GMO	5
	4	YES	GMO	5
	5	YES	GMO-free	5
GMO-free	6	YES	GMO-free	5
	7	YES	GMO-free	5
	8	YES	GMO-free	5
	9	YES	GMO-free + n-3 PUFA	5
GMO-free + n-3 PUFA	10	YES	GMO-free + n-3 PUFA	5
	11	YES	GMO-free + n-3 PUFA	5
	12	YES	GMO-free + n-3 PUFA	5
Non-PDO	13	NO	GMO	5
	14	NO	GMO	5
	15	NO	GMO	5
	16	NO	GMO	5
				Tot. 80

polyethylene bags and then transported under refrigeration to the laboratory. On the day of collection, visible connective and fat tissues were discarded from the muscle samples, while a sub-portion of the liver lobe (130–150 g) was chosen by cutting a vertical section, so as to include peripheral and central parts of the organ. Each sample was chopped, and sub-samples (20–30 g, representative of the bulk homogenized samples) were frozen at $-80\text{ }^{\circ}\text{C}$ for at least 24 h. Both matrices were then lyophilized for 24 h at $-55\text{ }^{\circ}\text{C}$ and 0.001–0.002 mbar pressure using a LyoQuest –55 Plus freeze-dryer (Telstar Co., Terrassa, Barcelona, Spain). After lyophilization, samples were finely pulverized using a plastic rod and stored at $+4\text{ }^{\circ}\text{C}$ until subsequent processing.

2.3. Reagents, solutions, and reference materials

Ultrapure water ($0.05\text{ }\mu\text{S cm}^{-1}$) obtained by the Milli-Q® purification system (Millipore, Bedford, USA) was employed for all analytical procedures and operations. TraceSelect® hydrogen peroxide (H_2O_2 , $\geq 30\%$ v/v, Fluka Chemie AG, Buchs, Switzerland) and sub-boiled, in-house prepared nitric acid (HNO_3) obtained from the distillation of Selectipur® HNO_3 (65% w/w, Lach-Ner, Neratovice, Czech Republic) by means of a Distillacid™ BSB-939-IR apparatus (Berghof, Eningen, Germany) were used throughout the mineralization of the samples.

Three multi-element calibration stock solutions were prepared at different concentrations from commercially available single- or multi-element standard solutions: solution I, containing Li, B, Al, V, Cr, Fe, Ni, Co, As, Se, Rb, Sr, Zr, Mo, Ru, Pd, Cd, Sn, Sb, Cs, Ba, Hf, Re, Pt, Tl, Pb, Bi: 10 mg L^{-1} (prepared from the 1 g L^{-1} Supelco ICP multi-element standard solution IV (Merck, Darmstadt, Germany) and single element standard solutions (1 g L^{-1} , Analytika Ltd., Prague, Czech Republic or SCP Science, Montreal, Canada); solution II, containing 1 mg L^{-1} of La, Ce, Pr, Nd, U: and 0.20 mg L^{-1} of Y, Tb, Ho, Yb, Sm, Eu, Gd, Er, Lu, and Dy (prepared from rare earth elements Astasol mix “M008”, Analytika Ltd., Prague, Czech Republic); solution III, containing Na, Mg, P, K, Ca, Mn, Cu, and Zn: 100 mg L^{-1} (prepared from 10 g L^{-1} single element standard solutions, Analytika Ltd., Prague, Czech Republic). A $200\text{ }\mu\text{g L}^{-1}$ Rh internal standard solution was prepared from a 1 g L^{-1} stock solution purchased from SCP Science (Montreal, Canada).

The following certified reference materials (CRMs) were analyzed: BCR® 184 Bovine muscle (Institute for Reference Materials and Measurements, IRMM, Geel, Belgium); BCR® 185 Bovine Liver (IRMM, Geel, Belgium); BCR® 422 Cod Muscle (IRMM, Geel, Belgium); CRM 12–2-01

Bovine Liver (pb-anal, Kosice, Slovakia); CRM 12–2-03 P-Alfalfa Essential and toxic elements in Lucerne (pb-anal, Kosice, Slovakia); CRM 12–2-04 Essential and Toxic Elements in Wheat Bread Flour (pb-anal, Kosice, Slovakia); GBW 10052 Green Tea (Chinese Academy of Geological Sciences, Beijing, China); NIST SRM 1577 Bovine Liver (National Institute of Science and Technology, NIST, Gaithersburg, MD, USA); NIST SRM 1666 Oyster Tissue (NIST, Gaithersburg, MD, USA); NCS ZC73015 Milk Powder (National Research Centre for Certified Reference Materials, NRCRM, Beijing, China).

2.4. Total mercury analysis

Freeze-dried samples and CRMs were directly analyzed for total Hg using a single-purpose atomic absorption spectrometer AMA-254 (Altec Ltd., Prague, Czech Republic), based on in situ dry ashing followed by gold amalgamation. Samples were weighed in a nickel boat and analyzed under the following conditions: first, samples were dried $120\text{ }^{\circ}\text{C}$ for 60 s. After that, samples underwent combustion in an oxygen atmosphere at a temperature of approximately $750\text{ }^{\circ}\text{C}$ for 150 s. The amalgamator was heated up to $900\text{ }^{\circ}\text{C}$ and the quantitative release of trapped mercury from the gold amalgamator to the measuring cuvette detection system took place at $900\text{ }^{\circ}\text{C}$ for 45 s. The absorbance of the peak area at 253.7 nm was monitored. The flow rate of the oxygen (99.5%) carrier gas was 170 mL/min .

2.5. ICP-MS multi-elemental analysis

Elements were measured following a tested and validated procedure previously published (Varrà, Husáková, Patočka, Ghidini, & Zanardi, 2021), which was slightly modified to be adapted to pig matrices. Briefly, about 100 mg of samples or CRMs were weighed and digested with a mixture of 1 mL of H_2O_2 (30% v/v) and 4 mL of HNO_3 (16% v/v). The mineralization program of the microwave oven (Speedwave™ MWS-3+ (Berghof, Eningen, Germany) featuring an output of 1450 W was set in three steps: i) 5 min of ramp-up time and 20 min of hold time at a temperature of $180\text{ }^{\circ}\text{C}$; ii) ramp to $220\text{ }^{\circ}\text{C}$ in 5 min and hold for 20 min ; iii) 5 min ramp and 5 min hold time at $100\text{ }^{\circ}\text{C}$. After cooling, the mineralized solutions were transferred to polypropylene volumetric flasks and brought to a volume of 25 mL with ultrapure water. An Agilent 7900 quadrupole ICP-MS instrument (Agilent Technologies, Inc., Santa Clara, CA, USA) with an octopole collision/reaction cell for polyatomic interference removal was used for multi-elemental analysis, using He as the collision gas at different collision energies. A detailed summary of the ICP-MS operating conditions is reported in Table 2. To correct for instrument instability and/or signal drift and non-spectral interferences (signal suppression or signal enhancement caused by the matrix) and to improve both precision and trueness of quantification, an internal standard solution containing $200\text{ }\mu\text{g L}^{-1}$ Rh was used in parallel with the liquid samples analyzed.

Multiple calibration standards ranging from 0 to $100\text{ }\mu\text{g L}^{-1}$ (Li, B, Al, V, Cr, Fe, Ni, Co, As, Se, Rb, Sr, Zr, Mo, Ru, Pd, Cd, Sn, Sb, Cs, Ba, Hf, Re, Pt, Tl, Pb, Bi), 0 to $10\text{ }\mu\text{g L}^{-1}$ (La, Ce, Pr, Nd, U), 0 to $2\text{ }\mu\text{g L}^{-1}$ (Y, Tb, Ho, Yb, Sm, Eu, Gd, Er, Lu, and Dy), and 0 to 10 mg L^{-1} (Na, Mg, P, K, Ca, Mn, Cu, and Zn) were prepared for the target elements by dilution from the 500 mg L^{-1} multi-element solution I, the $50 + 10\text{ mg L}^{-1}$ solution II, and the 100 mg L^{-1} solution III, respectively (see Section 2.3). Linear calibrations with a coefficient of determination >0.9999 were obtained for all elements.

2.5.1. Analytical performances

Quality assurance/quality control procedures were adopted throughout the analysis to assure the trueness and precision of the quantitative results. These procedures included the evaluation of the sensitivity of the method through the estimation of the detection limits of the method (MLODs) and the limits of quantification of the method (MLOQs) for each analyzed element (Table S1, Supplementary

Table 2

Analytical parameters and working conditions of ICP-MS for multi-element analysis of muscle and liver samples.

	Parameter	Type/Value
ICP	Plasma mode	General purpose
	Forward RF power (27 MHz) (W)	1550
	Sampling depth (mm)	10
	Nebulizer	Glass concentric, MicroMist
	Spray chamber	Scott quartz, Peltier-cooled at 2 °C
	Gas	Argon (99.999% purity)
	Nebulizer gas flow rate (L/min)	1.05
	Nebulizer pump (rps)	0.1
	Plasma gas flow rate (L/min)	15
	Auxiliary gas flow rate (L/min)	0.9
	Sampling cone	Nickel, i.d. 1 mm
	Skimmer cone	Nickel, i.d. 0.45 mm
	Mode	No Gas Helium High Energy Helium
	Extract 1 (V)	0
	Extract 2 (V)	-250 -245 -250
	Omega bias (V)	-100 -120 -110
	Omega lens (V)	9.7 12.7 12.3
MS Spec	Cell entrance	-30 -40 -140
	Cell exit	-50 -60 -150
	Deflect (V)	11.6 1.6 -60
	Plate bias	-35 -60 -150
	Helium flow (mL/min)	0 6 10
	OctP bias	-8 -18 -100
	OctP RF	200
	Energy discrimination (V)	5 5 5
	Number of elements	39 ^a 12 ^b 5 ^c
	Mode	Peak hopping
	Points per peak	1
Acquisition	Replicates	3
	Sweeps/replicate	100
	Acquisition time (s)	75

Monitored isotopes (integration time): ^a) ⁷Li, ⁹Be, ¹¹B, ²⁴Mg, ⁶⁶Zn, ⁸⁵Rb, ⁸⁸Sr, ⁸⁹Y, ⁹⁰Zr, ⁹⁵Mo, ¹⁰¹Ru, ¹⁰³Rh, ¹⁰⁵Pd, ¹¹¹Cd, ¹¹⁸Sn, ¹²¹Sb, ¹³³Cs, ¹³⁸Ba, ¹³⁹La, ¹⁴⁰Ce, ¹⁴¹Pr, ¹⁴⁶Nd, ¹⁴⁷Sm, ¹⁵³Eu, ¹⁵⁷Gd, ¹⁵⁹Tb, ¹⁶³Dy, ¹⁶⁵Ho, ¹⁶⁶Er, ¹⁷²Yb, ¹⁷⁵Lu, ¹⁷⁸Hf, ¹⁸⁵Re, ¹⁹⁵Pt, ²⁰⁵Tl, ²⁰⁶⁺²⁰⁷⁺²⁰⁸Pb, ²⁰⁹Bi, ²³²Th, ²³⁸U (all 0.1 s); ^b) ²³Na (0.3 s), ²⁷Al (0.1 s), ³⁹K, ⁴⁴Ca (both 0.3 s), ⁵¹V (1 s), ⁵²Cr, ⁵⁵Mn, ⁵⁶Fe, ⁵⁹Co, ⁶⁰Ni, ⁶³Cu, ¹⁰³Rh (all 0.3 s); ^c) ³¹P, ⁴⁹Ti, (both 0.1 s), ⁷⁵As, ⁷⁸Se (both 1 s), ¹⁰³Rh (0.3 s).

Material).

MLODs and MLOQs were calculated as that concentration equivalent to a signal of three and ten times, respectively, the standard deviation determined by measuring 10 replicates of a blank sample and considering the sample dilution factor.

In all cases, the MLODs were found to be significantly below the typical requirements for this analysis, so that the selected elements could be determined at the background level. Table S1 (Supplementary Materials) also summarizes the relative sensitivities of ICP-MS for the analysis of individual elements with the use of Rh ISTD.

The element quantification accuracy was evaluated using the above-mentioned CRMs (see Section 2.3). The high level of agreement between the target and the values found demonstrated the trueness of the data obtained (Supplementary Materials, Table S2). Intra-day and inter-day precisions were calculated to assess the overall precision of the method and were determined by analyzing individual CRMs three times during the same day and three different days over one month, respectively. The method was found to be precise enough due to the percent relative standard deviations (RSD%) of intra-day and inter-day precision, which were mostly below 10% (Supplementary Materials, Table S2).

2.6. Data processing and statistics

Triplicate measurements of elements resulting from ICP-MS and direct mercury analyses of individual pig muscle and liver samples were averaged and expressed as mean concentrations. Data were evaluated for homogeneity of variance and normal distribution by applying Box's M and Shapiro-Wilk's tests, respectively. Elemental data violating these assumptions (significance level of 5%) were corrected using the Box-Cox transformation. Initially, mean concentrations were utilized as inputs to construct radar charts, aiming to explore elemental trends. Transformed data were then analyzed by multivariate analysis of variance (MANOVA) to identify statistically significant differences among dependent elemental variables of the 4 groups of pig samples (i.e., conventional, GMO-free, GMO-free + n-3 PUFA, and non-PDO). A Tukey's post hoc test was used for multiple comparisons. The significant multivariate effects of elemental data on the membership of samples in the 4 groups was evaluated by Wilks' λ , Hotelling-Lawley Trace, Pillai's Trace, and Roy's Largest Root indexes. Statistically significant differences were identified at $p \leq 0.05$. Results of summary statistics of elemental concentrations (adjusted mean values, lower and upper 95% confidence intervals, CI) were expressed in the original scale of measurement after reversing the Box-Cox transformation (Meloun, Hill, Militký, & Kupka, 2000).

To attenuate the effect of high-magnitude variables and enhance the effect of low-magnitude variables, data were then scaled by mean subtraction and division by standard deviation. Six different clustering methods (single linkage, complete linkage, simple average, group average, median, and Ward's minimum variance) and 3 distance metrics (i.e., Euclidean, Manhattan and Pearson's correlation coefficient) were tested to define the best parameters for hierarchical cluster analysis (HCA). To this purpose, the cophenetic correlation coefficient was employed as a quality index. A coefficient closer to 1 indicated a higher efficiency of clustering (Saraçlı, Doğan, & Doğan, 2013). As a result, Ward's method (for clustering) and Pearson's correlation coefficient (as a distance measure for both samples and elemental variables) were selected for HCA, since they provided a cophenetic correlation coefficient of 0.9867 (Supplementary Materials, Table S3). The resulting cluster dendrograms and heatmaps of Pearson's correlation coefficient matrices were plotted to evaluate similarities and differences among samples and variables.

Multivariate analysis was used to investigate the existing relationships between the variables. A selection of the most informative variables was performed beforehand to simplify the final multivariate models. Indeed, a reduced model size is useful to improve prediction performances, speed of calculation, and data interpretability, as well as to reduce costs and time associated with the analysis. Neighborhood component analysis (NCA) was applied for this purpose. Briefly, NCA can automatically generate weights for each variable through the maximization of classification prediction accuracy based on Mahalanobis distance and the penalization of variables leading to misclassification results (Yang, Wang, & Zuo, 2012).

Elemental differences between the four groups of pig samples were thus assessed using soft independent modeling of class analogy (SIMCA) as a supervised class modeling technique. Briefly, SIMCA method relies on joint principal component analyses (PCAs), each one generated separately for the classes of interest to be modeled (Wold & Sjöström, 1977). Principal components (PCs) collecting variability within each class are hence defined independently and used to define the boundaries of a multivariate space to which the sample is accepted or refused to belong to. Acceptance or rejection is based on F-statistics resulting from the evaluation of the ratio between its squared distance from the model and the mean distance of the samples employed for model building. SIMCA models for the authentication of liver and muscle samples were generated using Box-Cox scaled data. The optimal number of PCs within each SIMCA model was defined based on the lowest root mean square error of cross-validation (RMSECV) calculated by leave-5-out cross-

validation.

All the statistical analyses were carried out using the software packages OriginPro 2021 (v. 9.8.0.200, Origin Lab Corporation, USA), MATLAB® R2022b (The MathWorks, Inc., MA, USA), and SIMCA (v. 16.0.2, Sartorius Stedim Data Analytics AB, Umea, Sweden).

Table 3

Mean and 95% confidence interval (CI, lower–upper)* concentrations ($\mu\text{g kg}^{-1}$, dry weight) of elements measured by means of ICP-MS in liver of heavy pigs from different groups.

	Conventional	GMO – free	GMO – free + n – 3 PUFA	Non – PDO
Ag	16 (10.7–26.3) ^a	13 (9.3–18.9) ^a	15 (11.8–18.7) ^a	11 (9.2–12.7) ^a
Al [#]	1.8 (1.44–2.25) ^a	1.6 (1.31–2.06) ^a	1.1 (0.095–1.116) ^b	1.3 (1.17–1.47) ^{ab}
As	27 (23.4–30.9) ^a	42 (36.2–49.1) ^b	32 (25.6–39.9) ^{ab}	42 (35.5–49.4) ^b
Ba	95 (80.7–112.2) ^a	113 (99.7–128.4) ^b	67 (60.0–76.4) ^c	84 (73.1–98.0) ^a
Be	0.4 (0.35–0.50) ^a	0.3 (0.29–0.37) ^b	0.3 (0.22–0.34) ^b	0.2 (0.17–0.32) ^b
Bi	0.2 (0.16–0.39) ^a	0.7 (0.49–1.05) ^b	0.5 (0.34–0.83) ^{ab}	0.2 (0.13–0.29) ^a
Ca [#]	178 (167–190) ^a	195 (180–209) ^{ab}	188 (176–200) ^{ab}	211 (195–228) ^b
Cd	147 (126–172) ^a	176 (152–205) ^a	81 (73.2–90.6) ^b	155 (131–182) ^a
Ce	5.6 (4.1–7.38) ^a	3.9 (3.15–5.05) ^a	2.6 (2.13–3.14) ^b	2.6 (2.2–3.1) ^b
Co	45 (38.0–52.8) ^a	46 (40.6–53.3) ^a	53 (44.4–63.4) ^a	33 (28.2–39.0) ^b
Cr	191 (144–265) ^a	188 (133–287) ^a	88 (79.3–98.3) ^b	183 (143–241) ^a
Cs	24 (20.2–27.6) ^a	30 (26.1–33.6) ^a	41 (36.7–45.9) ^b	48 (40.8–55.8) ^b
Cu [#]	38 (28.6–48.8) ^a	47 (36.0–62.0) ^a	38 (33.2–44.1) ^a	32 (26.7–38.6) ^a
Dy	0.2 (0.13–0.21) ^a	0.11 (0.087–0.128) ^b	0.08 (0.063–0.097) ^b	0.11 (0.098–0.122) ^b
Er	0.10 (0.075–0.119) ^a	0.05 (0.039–0.058) ^b	0.07 (0.058–0.077) ^{ab}	0.091 (0.075–0.107) ^a
Eu	0.14 (0.12–0.17) ^a	0.14 (0.128–0.172) ^a	0.09 (0.076–0.096) ^b	0.2 (0.15–0.22) ^a
Fe [#]	728 (635–834) ^a	486 (419–563) ^b	417 (359–486) ^b	389 (320–472) ^b
Gd	0.2 (0.13–0.21) ^a	0.09 (0.073–0.110) ^b	0.10 (0.089–0.117) ^b	0.11 (0.096–0.134) ^b
Hf	1.1 (0.98–1.35) ^a	3.8 (2.76–5.14) ^b	2.8 (2.04–3.74) ^b	1.0 (0.81–1.21) ^a
Hg [‡]	6.5 (5.46–7.66) ^a	4.7 (3.94–5.64) ^b	4.0 (3.21–4.92) ^b	3.8 (3.01–4.81) ^b
Ho	0.04 (0.028–0.044) ^a	0.02 (0.015–0.027) ^b	0.02 (0.017–0.025) ^b	0.03 (0.025–0.033) ^{ab}
K [#]	8487 (7782–9192) ^a	8396 (7899–8893) ^a	8396 (7973–8747) ^a	8697 (8182–9211) ^a
La	3.5 (2.77–4.51) ^a	2.1 (1.64–2.69) ^b	1.7 (1.49–2.04) ^b	1.9 (1.70–2.14) ^b
Li	1.3 (0.85–1.83) ^a	3.8 (3.18–4.48) ^b	6.4 (4.82–8.21) ^c	3.9 (2.93–5.01) ^b
Lu	0.03 (0.028–0.037) ^a	0.023 (0.0200–0.0262) ^b	0.012 (0.0094–0.0147) ^c	0.02 (0.015–0.026) ^b
Mg [#]	551 (482–555) ^a	532 (501–561) ^{ab}	540 (529–572) ^{ab}	582 (550–612) ^b
Mn [#]	7.5 (6.3–7.5) ^a	7.4 (6.96–7.81) ^{ab}	6.9 (6.05–7.93) ^{ab}	8.1 (7.53–8.65) ^b
Mo [#]	4.0 (3.6–4.2) ^a	4.3 (4.01–4.67) ^a	3.9 (3.74–4.26) ^a	4.1 (3.83–4.34) ^a
Na [#]	2012 (1831–2193) ^a	1950 (1780–2121) ^a	1979 (1880–2078) ^a	2058 (1937–2178) ^a
Nd	0.8 (0.60–1.03) ^a	0.4 (0.36–0.54) ^b	0.5 (0.43–0.55) ^b	0.5 (0.47–0.58) ^b
Ni	51 (39.2–65.5) ^a	72 (61.9–82.7) ^b	51 (45.0–57.0) ^a	83 (71.0–97.5) ^b
P [*]	9877 (8516–9952) ^a	9373 (8751–9956) ^a	9262 (9055–10,428) ^a	10,272 (9713–10,802) ^a
Pb	26 (19.8–35.6) ^a	17 (14.9–20.0) ^b	19 (17.9–21.1) ^{ab}	19 (17.8–21.3) ^{ab}
Pd	1.0 (0.70–1.43) ^a	5.7 (3.8–8.1) ^b	7.0 (5.41–8.87) ^b	1.8 (1.4–2.2) ^a
Pr	0.3 (0.20–0.36) ^a	0.14 (0.111–0.171) ^b	0.17 (0.160–0.191) ^{bc}	0.2 (0.18–0.22) ^{ac}
Pt	7.0 (5.76–8.75) ^a	8.0 (8.0–9.9) ^a	7.2 (6.27–8.35) ^a	7.7 (6.90–8.50) ^a
Rb [#]	18 (16.0–19.2) ^a	18 (16.8–19.6) ^{ab}	18 (17.0–19.8) ^{ab}	21 (19.6–22.2) ^b
Ru	0.05 (0.041–0.069) ^a	0.05 (0.034–0.063) ^a	0.06 (0.040–0.078) ^a	0.073 (0.048–0.112) ^a
Sb	1.5 (1.09–2.33) ^a	1.1 (0.95–1.20) ^a	0.6 (0.53–0.72) ^b	1.3 (0.64–1.01) ^b
Se	1483 (1364–1606) ^a	1645 (1502–1796) ^a	1657 (1573–1743) ^a	1572 (1453–1697) ^a
Sm	0.2 (0.19–0.31) ^a	0.16 (0.140–0.196) ^a	0.3 (0.19–0.35) ^a	0.2 (0.13–0.22) ^a
Sr	114 (102–127) ^a	127 (117–137) ^a	119 (107–132) ^a	126 (118–135) ^a
Tb	0.3 (0.20–0.32) ^a	0.3 (0.25–0.38) ^a	0.08 (0.053–0.113) ^b	0.3 (0.19–0.39) ^a
Te	1.1 (1.03–1.24) ^a	1.2 (1.05–1.41) ^a	1.3 (1.13–1.50) ^a	1.1 (0.92–1.31) ^a
Th	0.6 (0.50–0.71) ^a	1.5 (1.10–2.11) ^b	0.9 (0.66–1.34) ^b	0.5 (0.39–0.63) ^a
Ti	106 (94–119) ^a	79 (68.3–91.0) ^b	73 (65.7–79.9) ^b	89 (80.0–99.1) ^{ab}
Tl	0.7 (0.50–0.97) ^a	0.9 (0.68–1.07) ^{ab}	0.6 (0.44–0.72) ^a	1.2 (0.90–1.61) ^b
U	3.3 (2.34–4.70) ^a	1.4 (1.08–1.91) ^b	0.3 (0.23–0.37) ^c	1.3 (0.96–1.65) ^b
V	50 (38.4–66.0) ^a	26 (19.2–36.2) ^b	5.1 (4.22–6.07) ^c	21 (14.9–28.9) ^b
W	0.8 (0.52–1.14) ^a	4.1 (2.95–5.51) ^b	2.9 (2.06–4.05) ^b	0.5 (0.37–0.71) ^a
Y	1.7 (1.36–2.05) ^a	1.5 (1.19–1.83) ^a	0.9 (0.76–1.08) ^b	1.5 (1.37–1.73) ^a
Yb	0.1 (0.10–0.15) ^a	0.06 (0.046–0.076) ^b	0.06 (0.047–0.067) ^b	0.10 (0.075–0.127) ^a
Zn [#]	180 (176–223) ^a	177 (158–195) ^a	202 (148–192) ^a	210 (189–231) ^a
Zr	4.9 (4.03–5.94) ^{ab}	7.0 (5.76–8.53) ^a	5.5 (4.36–7.03) ^{ab}	4.2 (3.34–5.25) ^b

Data followed by different superscript letters are different at $p \leq 0.05$ according to the MANOVA results.

GMO-free: heavy pigs from Parma Ham Protected Designation of Origin circuit fed without the use of genetically modified feed; GMO-Free + n-3 PUFA: heavy pigs from Parma Ham Protected Designation of Origin circuit, fed without the use of genetically modified feed and supplemented with polyunsaturated fatty acids ingredients; non-PDO: heavy pigs outside the Parma Ham Protected Designation of Origin circuit.

* Means and 95% lower and upper CIs were calculated by reversing the Box-Cox transformed data.

Data are expressed in mg kg^{-1} (dry weights).

‡ Hg concentrations were measured by means of AMA-254 mercury analyzer.

† B, Re, Sn were excluded from liver matrix due to the high percentage (> 70%) of values below the MLODs.

3. Results and discussion

3.1. Concentrations and profiles of elements in heavy pig livers and muscles

The concentrations (on dry weight basis) of the measured elements in the four pig groups analyzed are detailed in Tables 3 and 4. Regardless the group, the most abundant muscular element was K, followed by P,

Table 4

Mean and 95% confidence interval (CI, lower–upper)^a concentrations ($\mu\text{g kg}^{-1}$, dry weight) of elements measured by ICP-MS in muscles of heavy pigs from different groups.

	Conventional	GMO-free	GMO-free + n-3 PUFA	Non-PDO
Ag	3.8 (2.9–5.2) ^a	5.8 (4.78–7.27) ^b	19 (13.3–28.3) ^c	15 (11.9–19.2) ^c
Al [#]	1.8 (0.92–1.43) ^a	1.2 (1.02–1.47) ^{ab}	1.1 (0.94–1.85) ^b	1.2 (0.99–1.45) ^a
As	23 (17.7–31.4) ^a	26 (17.6–39.4) ^a	31 (18.9–54.6) ^a	39 (31.4–48.8) ^a
B	627 (486–786) ^a	747 (637–866) ^a	395 (300–502) ^b	311 (219–419) ^b
Ba	239 (207–278) ^{ab}	215 (167–286) ^a	224 (202–251) ^{ab}	314 (289–344) ^b
Be	0.07 (0.055–0.092) ^a	0.4 (0.31–0.61) ^b	0.33 (0.23–0.48) ^b	0.12 (0.082–0.165) ^a
Bi	0.3 (0.22–0.29) ^a	1.2 (0.61–1.46) ^b	1.3 (0.98–1.79) ^b	0.4 (0.31–0.43) ^a
Ca [#]	175 (156–196) ^a	194 (167–286) ^a	199 (186–251) ^a	194 (181–208) ^a
Cd	1.8 (1.56–2.01) ^a	3.1 (2.48–3.90) ^b	2.6 (2.26–2.93) ^b	3.0 (2.71–3.44) ^b
Ce	2.5 (1.70–3.95) ^a	2.4 (2.48–3.90) ^a	4.4 (3.60–5.41) ^{ab}	7.0 (4.67–11.11) ^b
Co	2.6 (2.18–3.16) ^{ab}	3.0 (1.54–4.07) ^{ab}	3.8 (3.36–4.24) ^b	4.1 (3.44–5.08) ^b
Cr	184 (112–301) ^a	179 (143–223) ^a	162 (130–201) ^a	678 (420–1096) ^b
Cs	55 (48.0–62.1) ^a	59 (51.8–67.2) ^a	102 (93–112) ^b	118 (109–128) ^b
Cu [#]	4.9 (3.49–5.66) ^{ab}	4.2 (3.73–4.78) ^a	4.0 (3.48–5.39) ^{ab}	5.5 (4.81–6.35) ^b
Dy	0.06 (0.048–0.073) ^a	0.08 (0.065–0.091) ^a	0.07 (0.058–0.090) ^a	0.06 (0.044–0.069) ^a
Er	0.05 (0.042–0.060) ^a	0.06 (0.054–0.073) ^a	0.05 (0.034–0.068) ^a	0.03 (0.019–0.034) ^b
Eu	1.1 (0.78–1.52) ^a	0.7 (0.34–1.63) ^{ab}	0.4 (0.36–0.52) ^b	0.4 (0.29–0.44) ^b
Fe [#]	89 (67.1–90.3) ^a	74 (66.0–82.5) ^a	78 (81.1–97.9) ^a	87 (81.3–91.9) ^a
Gd	0.04 (0.034–0.058) ^a	0.05 (0.043–0.072) ^{ab}	0.08 (0.063–0.098) ^b	0.10 (0.073–0.129) ^c
Hf	1.0 (0.93–1.15) ^a	4.4 (3.23–5.91) ^b	3.0 (2.36–3.82) ^b	0.79 (0.65–0.96) ^a
Hg [§]	3.2 (2.41–4.62) ^a	3.1 (2.32–4.48) ^a	4.5 (3.82–5.35) ^b	1.87 (1.56–2.31) ^c
Ho	0.01 (0.0086–0.0122) ^a	0.02 (0.013–0.023) ^b	0.02 (0.015–0.025) ^b	0.01 (0.010–0.015) ^{ab}
K [#]	13,750 (10,439–12,563) ^a	12,580 (11,457–13,610) ^{ab}	11,550 (12,610–14,801) ^b	13,058 (12,410–13,676) ^{ab}
La	1.7 (1.26–2.38) ^a	1.7 (1.21–2.46) ^a	1.9 (1.55–2.35) ^{ab}	3.5 (2.52–4.49) ^b
Li	1.3 (0.96–1.71) ^a	3.2 (2.02–5.04) ^b	6.8 (5.41–8.53) ^c	4.0 (3.49–4.59) ^b
Lu	0.02 (0.015–0.028) ^a	0.03 (0.022–0.044) ^a	0.02 (0.017–0.025) ^a	0.012 (0.0093–0.0157) ^b
Mg [#]	742 (681–803) ^a	843 (756–931) ^a	806 (729–883) ^a	714 (676–753) ^a
Mn [#]	0.8 (0.74–0.91) ^a	0.6 (0.51–0.69) ^b	0.6 (0.49–0.67) ^b	0.8 (0.70–0.83) ^a
Mo [#]	0.09 (0.080–0.101) ^a	0.08 (0.068–0.089) ^a	0.08 (0.063–0.090) ^a	0.10 (0.087–0.104) ^a
Na [#]	2086 (1515–2883) ^a	1935 (1735–2145) ^{ab}	1695 (1530–2247) ^b	2055 (1920–2194) ^a
Nd	0.1 (0.09–0.21) ^a	0.3 (0.19–0.38) ^b	0.2 (0.21–0.30) ^b	0.24 (0.21–0.29) ^b
Ni	59 (45–78) ^{ab}	48 (43.4–54.5) ^a	66 (54.7–81.1) ^{ab}	88 (77.2–102.1) ^b
P [#]	6983 (6567–7948) ^a	7718 (6901–8534) ^a	7258 (6406–7559) ^a	6661 (6311–7010) ^a
Pb	7.4 (5.89–9.83) ^a	7.3 (6.31–8.44) ^a	12 (10.4–14.4) ^b	15 (12.1–18.8) ^b
Pd	0.8 (0.55–1.25) ^a	6.0 (4.48–7.92) ^b	5.4 (3.91–7.33) ^b	0.8 (0.49–1.24) ^a
Pr	0.06 (0.043–0.077) ^a	0.12 (0.083–0.171) ^b	0.11 (0.086–0.135) ^b	0.10 (0.079–0.119) ^b
Pt	8.7 (7.39–10.17) ^a	10 (8.5–11.7) ^a	9.7 (8.67–10.81) ^a	11 (9.7–13.2) ^a
Rb [#]	17 (15.3–20.6) ^a	16 (13.9–17.1) ^{ab}	14 (13.21–19.07) ^b	17 (16.0–18.3) ^a
Re	0.02 (0.014–0.025) ^a	0.14 (0.084–0.238) ^b	0.08 (0.035–0.173) ^b	0.02 (0.014–0.036) ^a
Ru	0.05 (0.040–0.069) ^a	0.2 (0.09–0.26) ^b	0.14 (0.083–0.230) ^b	0.06 (0.037–0.082) ^a
Sb	0.6 (0.23–1.05) ^a	0.07 (0.061–0.085) ^b	0.14 (0.11–0.33) ^b	0.02 (0.012–0.031) ^b
Se	520 (451–589) ^a	579 (506–652) ^a	596 (542–649) ^a	575 (537–612) ^a
Sm	0.05 (0.040–0.070) ^a	0.07 (0.056–0.096) ^{ab}	0.12 (0.093–0.173) ^b	0.08 (0.068–0.096) ^{ab}
Sn	1.4 (0.91–2.20) ^a	1.3 (0.93–1.91) ^a	4.5 (3.76–5.34) ^b	3.7 (3.1–4.4) ^b
Sr	190 (165–218) ^a	181 (155–211) ^a	171 (151–194) ^a	175 (153–200) ^a
Tb	1.9 (1.38–2.69) ^a	1.2 (0.61–2.82) ^{ab}	0.92 (0.77–1.11) ^{ab}	0.6 (0.51–0.78) ^b
Te	0.7 (0.56–0.78) ^a	1.3 (1.03–1.56) ^b	1.0 (0.81–1.24) ^b	0.5 (0.39–0.67) ^a
Th	0.4 (0.33–0.43) ^a	2.0 (1.40–2.79) ^b	1.8 (1.43–2.43) ^b	0.5 (0.45–0.65) ^a
Ti	66 (50–93) ^a	68 (55–87) ^a	78 (63.1–99.8) ^a	71 (59.4–87.0) ^a
Tl	0.4 (0.25–0.50) ^a	0.8 (0.63–1.05) ^b	0.7 (0.56–0.92) ^b	0.8 (0.59–1.04) ^b
U	0.1 (0.11–0.16) ^a	0.2 (0.17–0.32) ^b	0.2 (0.15–0.22) ^b	0.2 (0.18–0.24) ^b
V	2.7 (2.01–3.67) ^a	2.8 (2.29–3.59) ^a	2.0 (1.77–2.39) ^a	5.4 (3.9–7.9) ^b
W	1.1 (0.92–1.40) ^a	5.6 (4.25–7.42) ^b	4.8 (3.95–5.73) ^b	5.4 (4.1–7.0) ^b
Y	0.8 (0.63–1.11) ^{ab}	1.0 (0.77–1.26) ^a	0.9 (0.75–1.19) ^a	0.6 (0.50–0.73) ^b
Zn [#]	133 (123–151) ^a	129 (114–143) ^a	137 (122–144) ^a	134 (127–141) ^a
Zr	4.2 (3.50–5.16) ^a	9.1 (7.45–11.1) ^b	6.9 (5.8–8.1) ^b	4.0 (3.53–4.54) ^a

Data followed by different superscript letters are different at $p \leq 0.05$ according to the MANOVA results.

GMO-free: heavy pigs from Parma Ham Protected Designation of Origin circuit fed without the use of genetically modified feed; GMO-Free + n-3 PUFA: heavy pigs from Parma Ham Protected Designation of Origin circuit, fed without the use of genetically modified feed and supplemented with polyunsaturated fatty acids ingredients; non-PDO: heavy pigs outside the Parma Ham Protected Designation of Origin circuit.

^a Means and 95% lower and upper CIs were calculated by reversing the Box-Cox transformed data.

[#] Data are expressed in mg kg^{-1} (dry weights).

[§] Hg concentrations were measured by means of AMA-254 mercury analyzer.

Na, Mg, Ca, Zn, and Fe (Table 4). The same decreasing order of abundance was reported by other authors, although meat cuts different from the diaphragm were mainly considered in the literature (Bilge et al., 2016; García-Vaquero, Miranda, Benedito, Blanco-Penedo, & López-Alonso, 2011; Tomović et al., 2019; Zhao et al., 2023). Specifically, the concentrations of K and Na in pig muscles observed by Bilge and co-authors are consistent with the findings reported in this study (Bilge

et al., 2016). However, the concentrations of Ca and Zn were lower, with Zn being approximately half of the levels detected in the current investigation (Bilge et al., 2016).

P was the most abundant element found in the liver (Table 3). The less abundant elements ($\mu\text{g kg}^{-1}$ range) were Er, Ho, Lu, and Ru in the liver, and Dy, Er, Gd, Ho, Lu, Mo, Pr, Re, Ru, and Sm in the muscle (Tables 3 and 4, respectively). Concentrations of trace elements are

mostly in close agreement with data reported by other authors (Parinet et al., 2018; Tomović et al., 2019; Zhao et al., 2023), although the specific comparison of rare earth elements (REEs) values with literature was difficult because of a lack of data. Concentrations of potentially toxic metals (As, Cd, Pb, and Hg) were very low both in muscle and liver tissues and similar to those found across Europe (Dehelean, Cristea, Puscas, Hategan, & Magdas, 2022; López-Alonso et al., 2007; Parinet et al., 2018).

To better elucidate the distribution patterns of elements, a ratio analysis between elemental concentrations in the livers and in the muscles was performed. As expected, all groups of pigs showed a marked accumulation of Cd, Mo, Co, Cu, Fe, and Mn in the liver (Fig. 1). All these elements tend to be selectively stored in the kidney and liver of mammals due to their high binding affinity to metallothioneins, of which these organs are richer compared to skeletal muscles (Miles, Hawksworth, Beattie, & Rodilla, 2000). As, Bi, Hg, Pb, and Zn have also a very strong affinity to metallothioneins, but no hepatic accumulation was observed in this work (Fig. 1). The GMO-free pig group also showed a higher accumulation degree of Ag, Be, Gd, Nd, Pr, Sm, U, and V in the liver, whereas the remaining pig groups exhibited comparatively lower accumulation levels (Fig. 1). On the other side, Ba, Eu, and Tb were slightly more abundant in the muscle of all the pig groups.

3.1.1. Radar charts and multivariate analysis of variance (MANOVA)

For a simple and rapid overview of potential different multi-elemental signatures, mean concentrations were plotted in radar charts (Fig. 2.). To simplify interpretation of the results, radar charts were generated independently for macro-, micro-, and trace elements (REEs on their own). The elemental profiles of both pig matrices varied markedly among the 4 groups of pigs. For instance, non-PDO liver samples presented clearly different patterns of the macro-elements P, K, Na, Mg, Zn, Ca, Rb, and Mn, which were more abundant compared to other groups (Fig. 2A). All these elements were not a mark of distinction for non-PDO muscle samples (Fig. 2B). On the contrary, micro- and trace-elements such as Ba, Cd, Hf, and Zr were a feature for both liver and muscle samples of the GMO-free group (Fig. 2A, Fig. 2B). Conventional samples presented a unique distribution of REEs, particularly evident in the liver (Fig. 2A). Concentrations of Er in the muscle were more pronounced in GMO-free samples, while those of Li, Ho, and Yb became more indicative of the GMO-free + n-3 PUFA sample group (Fig. 2B). Li, as well as Pd, and Te, were found to have a different distribution pattern also in the liver of the GMO-free+ n-3 PUFA group (Fig. 2A). However, the direct comparison of multi-elemental signatures between the two tissues using only the radar charts was hindered by the absence of well-defined patterns in the livers or in the muscles of the

same pig group.

A detailed investigation of elemental differences among the four groups of pigs was further performed by MANOVA. According to the Wilks' Lambda, Hotelling-Lawley Trace, Pillai's Trace, and Roy's Largest Root indexes, the presence of a significant multivariate effect of pig groups on the elemental content existed ($p \leq 0.05$) (Supplementary Material, Table S4). The 4 groups of pigs were not found to be all statistically different from each other for all the elements measured. By analyzing groups one by one, it emerged that most of the differences concerned trace and ultra-trace elements, while few significant differences were observed for macro- and micro-elements. A summary of the results from the MANOVA test followed by Tukey's post-hoc test for pairwise comparison among elemental concentration of groups of pig liver and muscle samples is reported in Tables 3 and 4, respectively. The exact p values resulting from the above statistics are detailed in Table S5 and S6 of the Supplementary Material.

The GMO-free and GMO-free + n-3 PUFA groups were together different from conventional and non-PDO groups due to the hepatic concentrations of Hf, Pd, Th, W, and Yb ($p \leq 0.05$, Table 3) and the muscular concentrations of Be, Bi, Hf, Pd, Re, Ru, Te, Th, and Zr ($p \leq 0.05$, Table 4). Mn was also an inorganic descriptor of GMO-free and GMO-free + n-3 PUFA pigs since its concentrations were significantly lower in these groups of samples ($p \leq 0.05$, Table 4). As for the GMO-free + n-3 PUFA samples alone, these were significantly more depleted of Ba, Cd, Cr, Eu, Lu, V, and Y in the liver and more enriched in Li both in the liver and in the muscle ($p \leq 0.05$, Tables 3 and 4, respectively), as already observed in the radar charts. These results are in contrast with previous findings, which suggested a higher degree of Cd accumulation in goats receiving feedstuffs supplemented with flaxseed and of Cr in growing pigs fed with flaxseed oils (Sawosz et al., 2001). Nonetheless, because other studies have described flax as an excluder plant for Cd, the decreased Cd concentration observed in the liver tissues of GMO-free + n-3 PUFA pigs may be attributed to a potential low Cd contamination in the flaxseed administered to animals (Saleem et al., 2020).

Samples from the non-PDO group stand out from the other groups for significantly lower concentrations of Co in the liver ($p \leq 0.05$, Table 3 and Supplementary Material, Table S5), as well as higher concentrations of Cr, Gd, and V, and lower concentrations of Er, Hg, and Lu in the muscle ($p \leq 0.05$, Table 4 and Supplementary Material, Table S6). In this regard, Co has been recently identified as a marker for the discrimination between pork meat samples coming from intensive and home-breeding farms (Cristea, Voica, Feher, Puscas, & Magdas, 2022). Although the animals analyzed in the current study were all from industrial and intensive farming, it cannot be ruled out that the observed variation of Co amount in the liver of non-PDO samples could still be an

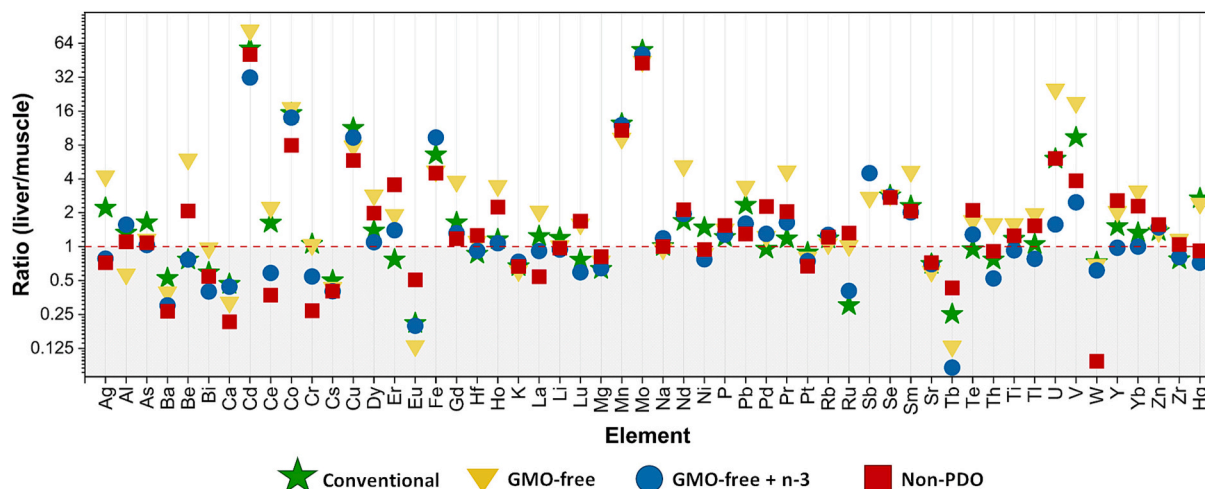


Fig. 1. Ratio of pig liver to pig muscle mean concentrations (Box-Cox reversed) of the measured elements.

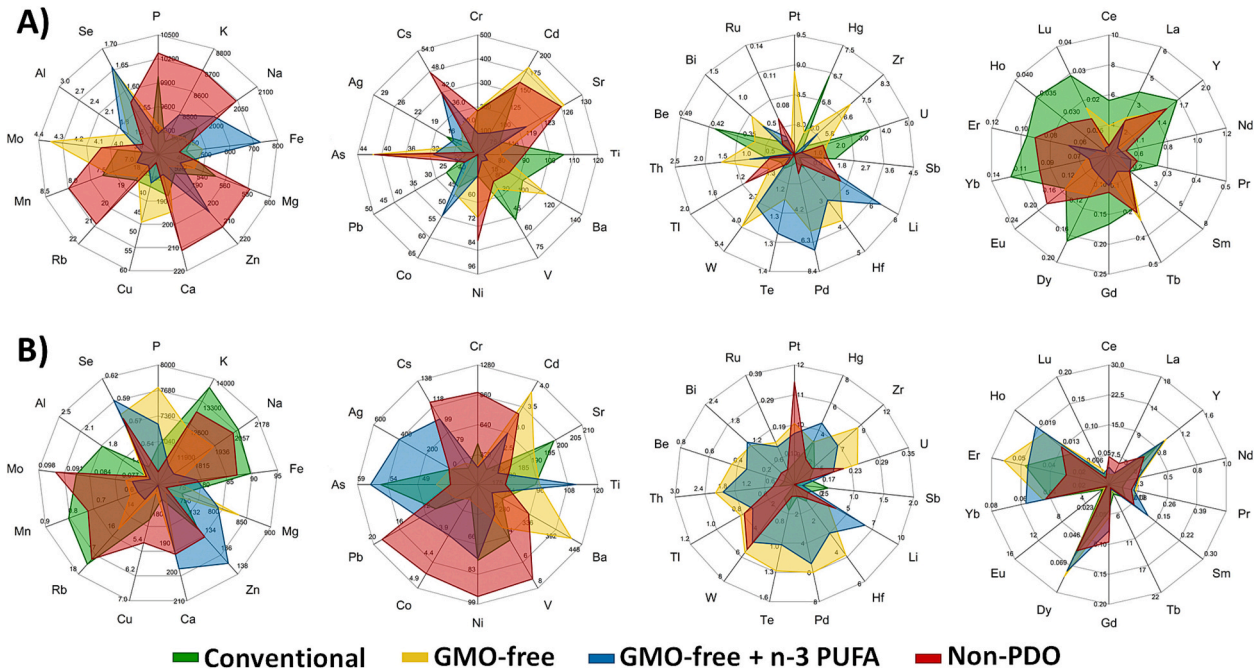


Fig. 2. Radar plots showing mean concentrations patterns of elements (REEs profiles plotted separately) measured in livers (A) and muscles (B) of the four groups of heavy pigs.

indicator of the different breeding and feeding regimes of these animals.

3.2. Grouping by hierarchical cluster analysis (HCA)

Clustergrams resulting from HCA application to the liver and muscle datasets are plotted in Fig. 3A and Fig. 3B, respectively. Samples and elements were ordered according to their similarity degree, identified by the length of the linkage connecting them, and assessed using Pearson's coefficients as a distance metric.

Globally, both samples and elements of liver and muscle datasets were divided into 3 major clusters. As for liver clustergram (Fig. 3A), the first major sample cluster was very homogeneous and included conventional samples and only 1 GMO-free + n-3 PUFA sample, whose grouping was primarily driven by higher concentrations of the first and the third sets of elements, including some REEs as La, Ce, Pr, and Nd. One sub-cluster, however, showed marked similarities due to high concentrations of Zr, Pd, Hf, Th, W, Bi, and Te. Compared to other REEs,

La and Ce can be easily mobilized and accumulated in different plants (Tsagkaris et al., 2021). For this reason, these elements are strongly indicative of the geographical area of provenance of crops and, by extension, of the feed ingredients employed, which, being supplied from the global market, tend to be relatively homogeneous and constant over time (Danezis et al., 2017). The second cluster of liver samples was very heterogeneous and included the majority of the non-PDO livers together as well as some samples of the other 3 pig groups. The third cluster encompassed the majority of the GMO-free and GMO-free + n-3 PUFA samples and the 4 remaining non-PDO samples. In this case, the clustering was strongly driven by the higher contributions of the elements of the second set (Be, Fe, V, U, Cd, Y, Yb, Lu, Ti, Gd, Dy, Ho, Er, Co, Ru, Eu, Tb, Cu, Zn, and Hg).

HCA applied to muscles (Fig. 3B) revealed a first cluster including GMO-free and GMO-free + n-3 PUFA samples (with only one conventional sample), for which the toxic metals Hg, As, Cd, and Pb had a strong contribution. The second smaller cluster encompassed part of the

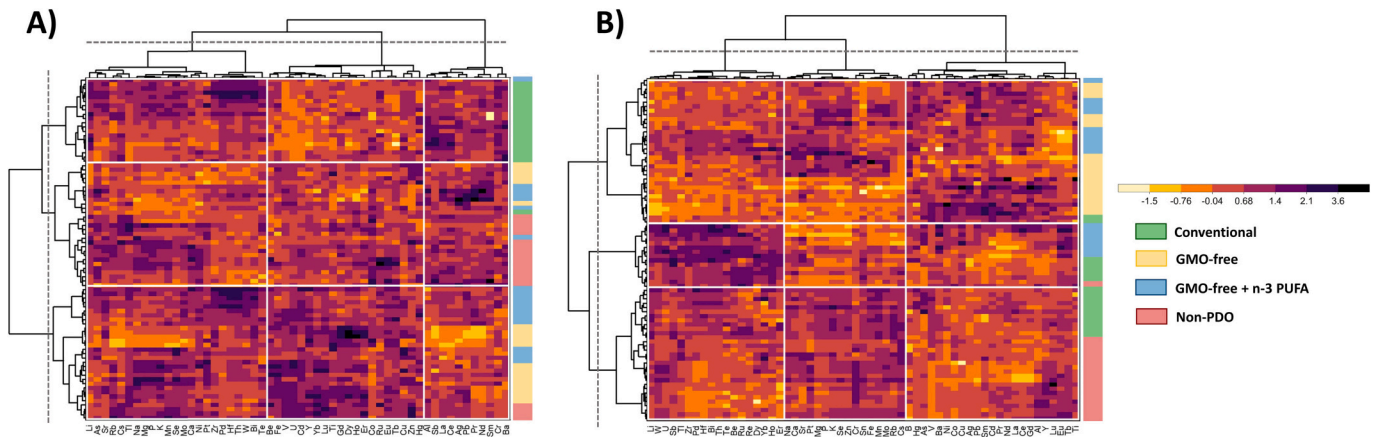


Fig. 3. Double dendrograms combined with heatmaps from HCA of pig liver (A) and muscle (B) datasets, showing the relationships among elemental concentrations (columns) and samples (rows). The colour scale of heatmaps is mapped to minimum-maximum concentration ranges of elements (Box-Cox transformed and standardized data).

conventional and the GMO-free + n-3 PUFA muscles (with only one non-PDO sample), which were better represented by elements of the first set (Li, W, U, Sb, Tl, Zr, Pd, Hf, Bi, Th, Te, Be, Ru, Re, Dy, Yb, Ho, and Er). Many of these elements were already identified as chemical descriptors of the GMO-free and the GMO-free + n-3 PUFA using radar charts and univariate data analysis (see Section 3.1). In addition, the potential of Li, W, Tl, Dy, and Er as good markers of the geographical origin of cheeses has been recently reported (Danezis et al., 2020). Finally, the third cluster was formed by the majority of non-PDO samples and fewer conventional ones, for which the concentrations of many macroelements had an important contribution.

In summary, the best clustering groups were conventional liver samples (Fig. 3A) and non-PDO muscle samples (Fig. 3B), while the most confused clusters included GMO-free and the GMO-free + n-3 PUFA liver or muscle samples. The high degree of overlapping between these samples might be the consequence of very comparable farming management practices.

Based on the above, it should be no surprise that an unclear situation concerning similarity among sample groups and elements mostly implicated in their differentiation emerged from univariate and unsupervised multivariate statistics. The power of supervised multivariate data analysis was hence exploited with the purpose of obtaining a more in-depth understanding of the data.

3.3. Modeling Italian heavy pig groups by SIMCA analysis

According to the results of the NCA, only 34 and 25 selected elements were used as predictors variables for the development of SIMCA models to authenticate liver and muscle samples of the different pig groups, respectively: Li, Na, Al, P, V, Cr, Fe, Ni, Co, Cu, Zn, As, Se, Rb, Sr, Pd, Ag, Cd, Cs, Ba, La, Ce, Pr, Nd, Er, Lu, Hf, W, Pt, Tl, Pb, Bi, Th, and U (liver); Li, Be, Mg, V, Co, As, Se, Sr, Zr, Mo, Ag, Cd, Sn, Cs, Pr, Tb, Er, Hf, W, Re, Pt, Tl, Bi, Th, and Hg (muscle). The SIMCA technique has already demonstrated its robustness as a reliable approach in authenticity studies concerning foods of animal origin, achieving up to 100% accuracy even with a reduced number of variables and successfully resolving complex issues such as the differentiation between conventional and organic production methods (Borges et al., 2015).

Three principal components (PCs) explaining 72%, 71%, and 69% of the overall variability (R^2X) present in the elemental profiles and encompassing 47%, 45%, 31%, and 38% of the predictive power (Q^2X) were extracted from the disjoint PCA models built for conventional, GMO-free, GMO-free + n-3 PUFA, and non-PDO livers, respectively. Similar results were obtained when fitting disjoint PCA models to the muscle dataset. Three PCs (for conventional and GMO-free + n-3 PUFA muscles) and 5 PCs (for GMO-free and non-PDO muscles) were required to fit the models, leading to R^2X values higher than 70% and Q^2X values higher than 40% in all the tested classes.

When plotting the cross-validated results of sample classification in

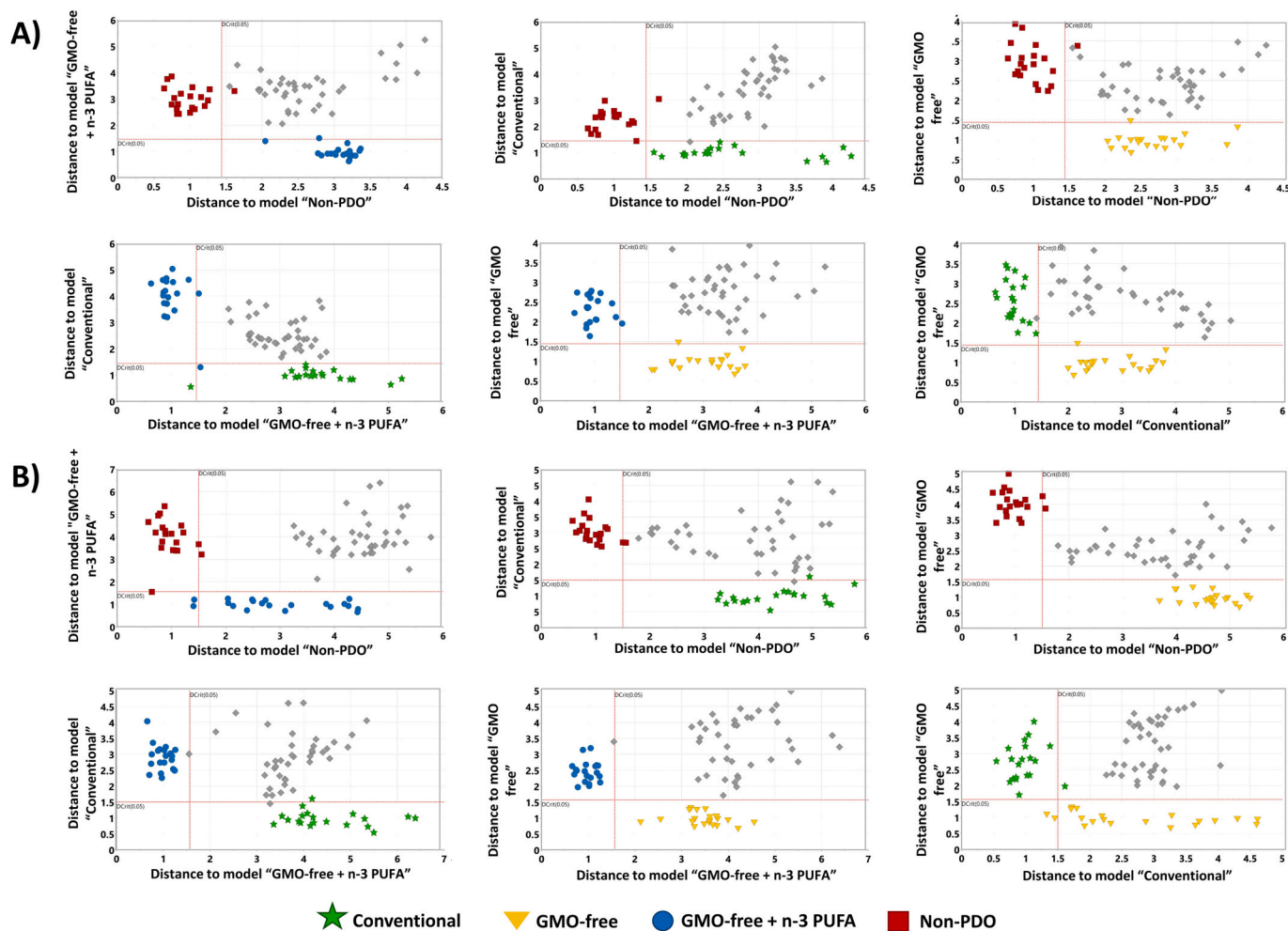


Fig. 4. Coomans' plots of the SIMCA models (Box-Cox transformed and scaled data) for livers (A) muscles (B) of pigs from different groups. Dotted red lines indicate critical distances (DCrit, 95% tolerance intervals) for each group of samples (grey diamond samples = samples from other classes). (For interpretation of the references to colour in this figure legend, the reader is referred to the web version of this article.)

Cooman's plots (Fig. 4), both liver (Fig. 4A) and muscle (Fig. 4B) samples were found to be sufficiently far from the critical distance lines (DCrit = 0.05) separating different pairwise classes and, therefore, to the point that a satisfying degree of separation was achieved. Nevertheless, it emerged that the classification results of cross-validated SIMCA analyses were less accurate for the muscle dataset (91% correct classification rate) than for the liver dataset (95% correct classification rate), as summarized in confusion matrices reported in Table 5. Across these results, it was found that one GMO-free + n-3 PUFA liver sample was wrongly recognized as conventional, while one conventional sample was ambiguously assigned both to the correct and the GMO-free + n-3 PUFA classes. Similarly, two non-PDO liver samples were recognized as belonging to none of the classes and to both the non-PDO and conventional classes, respectively.

The SIMCA models created for the GMO-free and GMO-free + n-3 PUFA muscles posed the greatest challenge for interpretation, as four samples were assigned to both the correct and non-correct classes. Consequently, these models exhibited higher confusion compared to the others created. This can be easily observed in Fig. 4B, where GMO-free and GMO-free + n-3 PUFA muscles distributed outside their delimitation areas and fell inside the area shared between two different classes.

In summary, although an overall 100% correct classification rate was not achieved even when SIMCA models were built using liver elemental profiles, the outcomes achieved when applying SIMCA to this tissue can be considered more than satisfactory. It should be noted that the classification accuracy was slightly lower for muscle tissue in comparison to liver tissue. This difference can be attributed to the higher concentrations and greater variability observed in the liver for the majority of the analyzed elements. As a result, the elemental profile of the swine liver tissue enabled a more accurate differentiation among groups of pigs, leading to improved classification performances. Despite these considerations, the achieved accuracy of 91% in authenticating pig groups using elemental profiles of muscle tissue can still be regarded as a significant and satisfactory outcome within the specific context of this study.

3.3.1 Modeling power of elements.
The impact of each element in describing the classes under investigation and building the SIMCA models was evaluated by examining the modeling power (MP) scores. MP scores were calculated by comparing the residual standard deviation with the corresponding data standard deviation of each variable. The values for this metric range from 0 to 1, where 0 indicates no MP and 1 indicates excellent MP (Wold & Sjöström, 1977). A threshold value of 0.5 was chosen to classify variables having a significant MP, which are graphically summarized in Fig. 5.

The elements showing the greatest MP and, hence, contributing the most to the separation of the sample by class membership were as follows: P > Rb > U > Th > Se (liver) and Se > Th > W > Mg (muscle) for conventional models; Hf > W > Bi > Th > Pd (liver) and Th > Bi > Hf > W (muscle) for GMO-free models; Pd > Fe > Li > Rb (liver) and Th > Bi > Sr > Pr (muscle) for GMO-free + n-3 PUFA models; V > U > Rb > Co (liver) and Tl > Cs > W > V (muscle) for non-PDO models. Previous studies focusing on the traceability of pork (Cristea et al., 2022) and beef products (Franke, Haldimann, Baumer, Hadorn, & Kreuzer, 2007; Heaton, Kelly, Hoogewerff, & Woolfe, 2008) have found Rb as a marker for traceability. Further, also Fe has been previously reported as an indicator for discriminating pigs raised in high-altitude areas (Zhao et al., 2023), as well as Sr, Fe, and Se for characterizing beef of different origins (Heaton et al., 2008).

As it can be observed, many of the elements with the highest MP were shared among all the different pig groups. The variables that exclusively distinguished the conventional samples were La, Ce, and Pb (for the liver model) and Er (for the muscle model). Furthermore, a high MP of Li was found exclusively for the model of muscles of GMO-free pigs. La and Ce were already identified as elements driving clustering of conventional livers by HCA (see Section 3.2). The elements which exclusively influenced the separation of GMO-free + n-3 PUFA class from the other classes were Li, Cr, Fe, As, and Sr (for the liver models) and Cd (for the muscle models), with the influence of Li and Cd already highlighted by the MANOVA results (see Section 3.1.1). Finally, potential unique markers for the non-PDO class were Lu (liver) and As and Mo (muscle).

In conclusion, the results reported in this study provide evidence supporting the potential use of multi-elemental signatures for discriminating different Italian heavy pig groups. Nonetheless, wider studies integrating many areas of knowledge, such as environmental chemistry, animal physiology, and nutrition science, would be required to find the underlying reason why tissues from each certified pig supply chain presented their distinctive multi-elemental signatures.

4. Conclusions

Several analytical techniques based on spectroscopy and mass-spectrometry have been suggested in the past to characterize meat products and authenticate their labeling claims. In this work, we propose for the first time a new method based on the combination of the multi-elemental profile of swine tissues with chemometrics, which demonstrated a high potential to distinguish specific value-added pig

Table 5

Misclassification tables resulting from cross-validation of SIMCA applied to liver and muscle elemental profiles of Italian heavy pigs from different groups.

	N. of samples	Correct	Conventional	GMO-free	GMO-free + n-3 PUFA	Non-PDO	No class	Multiclass
Livers								
Conventional	20	95%	19	0	0	0	0	1 ^a
GMO-free	20	100%	0	20	0	0	0	0
GMO-free + n-3 PUFA	20	95%	1	0	19	0	0	0
Non-PDO	20	90%	0	0	0	18	1	1 ^b
Total	80	95%	20	20	19	18	1	2
Muscles								
Conventional	20	95%	19	0	0	0	1	0
GMO-free	20	90%	0	18	0	0	0	2 ^c
GMO-free + n-3 PUFA	20	90%	0	0	18	0	0	2 ^d
Non-PDO	20	90%	0	0	0	18	1	1 ^e
Total	80	91%	19	18	18	18	2	5

PDO: heavy pigs from Parma Ham Protected Designation of Origin circuit; GMO-free: heavy pigs from Parma Ham Protected Designation of Origin circuit fed without the use of genetically modified feed; GMO-Free + n-3 PUFA: heavy pigs from Parma Ham Protected Designation of Origin circuit, fed without the use of genetically modified feed and supplemented with polyunsaturated fatty acids ingredients; Non-PDO: heavy pigs outside the Parma Ham Protected Designation of Origin circuit).

^a Both Conventional and PUFA (n = 1).

^b Both non-PDO and conventional (n = 1).

^c Both GMO-free and Conventional (n = 2).

^d Both GMO-free + n-3 PUFA and non-PDO (n = 2).

^e Both non-PDO and GMO-free + n-3 PUFA (n = 1).

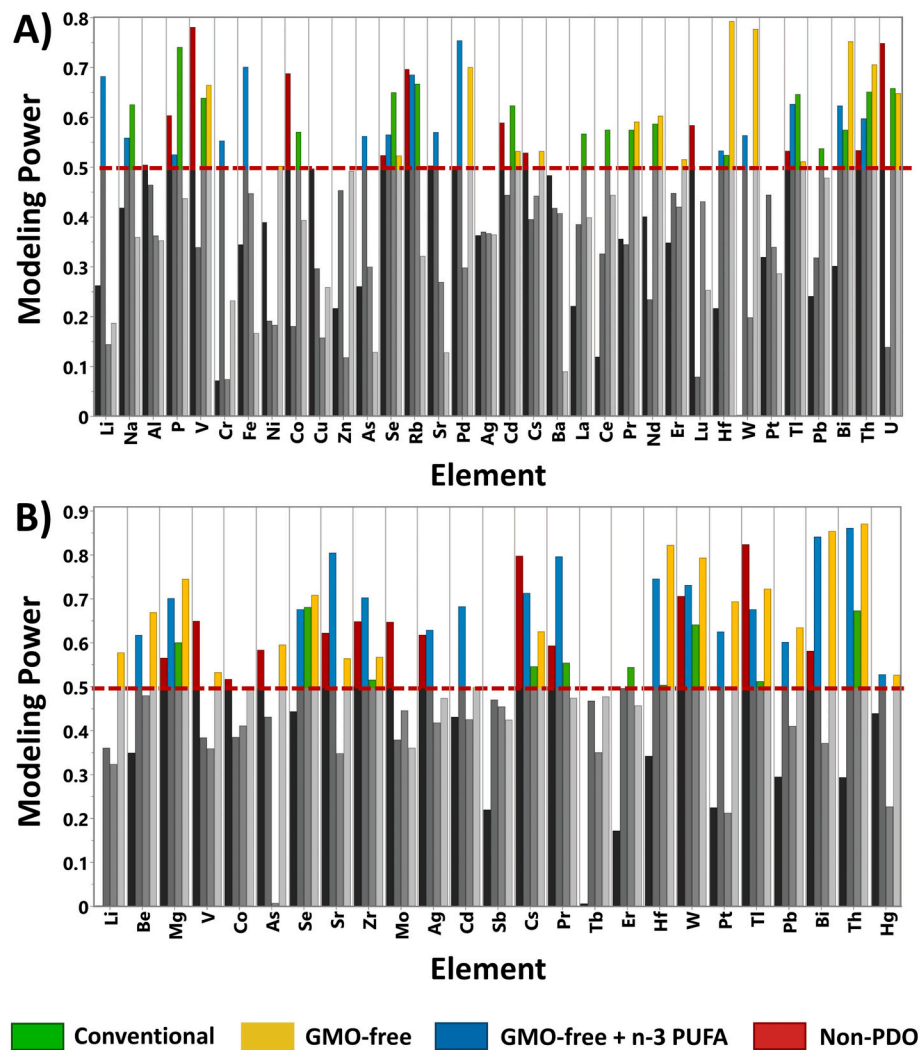


Fig. 5. Plots of the modeling power (MP) of each element for the SIMCA classification of pig liver (A) and muscle (B) samples belonging to the different groups. Dotted red lines indicate thresholds for influent MP values ($MP \geq 0.5$). Non-influent variables are represented by grey bars below the 0.5 MP threshold line, while influent variables are indicated by colored bars equal to or above the 0.5 MP threshold line. (For interpretation of the references to colour in this figure legend, the reader is referred to the web version of this article.)

meat obtained from the PDO Parma Ham production chain, going beyond the sole identification of the provenance and farming method of meat. In particular, the complementarity and richness of the chemical information enclosed within pig liver can be successfully exploited to verify the truthfulness of pig meat labels claiming the use of GMO-free and GMO-free plus n-3 PUFA feeds along the supply chain.

In view of the encouraging results achieved and the sensitivity, specificity, and robustness of the approach, the method proposed above is worth being further refined as a forthcoming analytical tool to deter potential fraud affecting the certified meat sectors.

In conclusion, it is recommended to explore the future development of conversion factors based on elemental profiles of raw offal and muscle tissues to match those observed in various processed meat products. Such advancements would be highly valuable for the inspection and verification of the authenticity of meat, both before or after its transformation, providing the benefit of using more readily available and affordable samples while eliminating the necessity of sampling costly meat cuts.

Funding

This work was supported by the Italian Ministry of Health (Project CLASSIFYFARM), the University of Pardubice (Grant No. SGS_2022_002), and the University of Parma (National Recovery and Resilience Plan (NRRP), Mission 4 Component 2 Investment 1.3 - Call for tender No. 341

of 15/03/2022 of Italian Ministry of University and Research funded by the European Union – NextGenerationEU. Award Number: Project code PE0000003, Concession Decree No. 1550 of 11/10/2022 adopted by the Italian Ministry of University and Research, CUP D93C22000890001, Project “Research and innovation network on food and nutrition Sustainability, Safety and Security – Working ON Foods” (ONFoods)).

CRediT authorship contribution statement

Maria Olga Varrà: Investigation, Data curation, Writing – original draft. **Lenka Husáková:** Methodology, Data curation, Validation, Writing – review & editing. **Emanuela Zanardi:** Project administration, Supervision, Validation, Writing – review & editing. **Giovanni Loris Alborali:** Funding acquisition, Methodology. **Jan Patočka:** Methodology. **Adriana Ianieri:** Funding acquisition, Resources. **Sergio Ghidini:** Conceptualization, Writing – review & editing.

Declaration of Competing Interest

The authors declare that they have no known competing financial interests or personal relationships that could have appeared to influence the work reported in this paper.

Data availability

The dataset generated during the current study will be made

available on reasonable request.

Appendix A. Supplementary data

Supplementary data to this article can be found online at <https://doi.org/10.1016/j.meatsci.2023.109285>.

References

- Amici, A., Danieli, P. P., Russo, C., Primi, R., & Ronchi, B. (2012). Concentrations of some toxic and trace elements in wild boar (*Sus scrofa*) organs and tissues in different areas of the province of Viterbo, Central Italy. *Italian Journal of Animal Science*, 11 (4), Article e65. <https://doi.org/10.4081/ijas.2011.e65>
- Barone, G., Storelli, A., Quaglia, N. C., Garofalo, R., Meleleo, D., Busco, A., & Storelli, M. M. (2021). Trace metals in pork meat products marketed in Italy: Occurrence and health risk characterization. *Biological Trace Element Research*, 199 (8), 2826–2836. <https://doi.org/10.1007/s12011-020-02417-z>
- Bartkovský, M., Sopková, D., Andrejčáková, Z., Vlčková, R., Semjon, B., Marcinčák, S., ... Kyzeková, P. (2022). Effect of concentration of flaxseed (*Linum usitatissimum*) and duration of administration on fatty acid profile, and oxidative stability of pork meat. *Animals*, 12(9). <https://doi.org/10.3390/ani12091087>
- Bilge, G., Velioglu, H. M., Sezer, B., Eseller, K. E., & Boyaci, I. H. (2016). Identification of meat species by using laser-induced breakdown spectroscopy. *Meat Science*, 119, 118–122. <https://doi.org/10.1016/j.meatsci.2016.04.035>
- Blanco-Penedo, I., López-Alonso, M., Miranda, M., Hernández, J., Prieto, F., & Shore, R. F. (2010). Non-essential and essential trace element concentrations in meat from cattle reared under organic, intensive or conventional production systems. *Food Additives and Contaminants - Part A Chemistry, Analysis, Control, Exposure and Risk Assessment*, 27(1), 36–42. <https://doi.org/10.1080/02652030903161598>
- Borges, E. M., Volmer, D. A., Gallimberti, M., de Souza, D. F., de Souza, E. L., & Barbosa, F. (2015). Evaluation of macro- and microelement levels for verifying the authenticity of organic eggs by using chemometric techniques. *Analytical Methods*, 7 (6), 2577–2584. <https://doi.org/10.1039/C4AY02986K>
- Bosi, P., & Russo, V. (2004). The production of the heavy pig for high quality processed products. *Italian Journal of Animal Science*, 3(4), 309–321. <https://doi.org/10.4081/ijas.2004.309>
- Chalabis-Mazurek, A., Valverde Piedra, J. L., Muszynski, S., Tomaszewska, E., Szymanczyk, S., Kowalik, S., ... Schwarz, T. (2021). The concentration of selected heavy metals in muscles, liver and kidneys of pigs fed standard diets and diets containing 60% of New Rye varieties. *Animals*, 11, 1377. <https://doi.org/10.3390/ani11051377>
- Cristea, G., Voica, C., Feher, I., Puscas, R., & Magdas, D. A. (2022). Isotopic and elemental characterization of Romanian pork meat in corroboration with advanced chemometric methods: A first exploratory study. *Meat Science*, 189, Article 108825. <https://doi.org/10.1016/j.meatsci.2022.108825>
- Danezis, G. P., Pappas, A. C., Tsiplakou, E., Pappa, E. C., Zacharioudaki, M., Tsgarkis, A. S., ... Georgiou, C. A. (2020). Authentication of Greek protected designation of origin cheeses through elemental metabolomics. *International Dairy Journal*, 104, Article 104599. <https://doi.org/10.1016/j.idairyj.2019.104599>
- Danezis, G. P., Pappas, A. C., Zoidis, E., Papadomichelakis, G., Hadjigeorgiou, I., Zhang, P., ... Georgiou, C. A. (2017). Game meat authentication through rare earth elements fingerprinting. *Analytica Chimica Acta*, 991, 46–57. <https://doi.org/10.1016/j.aca.2017.09.013>
- Dehelean, A., Cristea, G., Puscas, R., Hategan, A. R., & Magdas, D. A. (2022). Assigning the geographical origin of meat and animal rearing system using isotopic and elemental fingerprints. *Applied Sciences*, 12(23). <https://doi.org/10.3390/app122312391>
- Dugan, M. E. R., Vahmani, P., Turner, T. D., Mapiye, C., Juárez, M., Prieto, N., ... Aalhus, J. L. (2015). Pork as a source of omega-3 (n-3) fatty acids. *Journal of Clinical Medicine*, 4(12), 1999–2011. <https://doi.org/10.3390/jcm4121956>
- European Commission. (2013a). Commission Implementing Regulation (EU) No 1208/2013 of 25 November 2013 approving minor amendments to the specification for a name entered in the register of protected designations of origin and protected geographical indications (Prosciutto di Parma (PDO)). *Official Journal of the European Union*, L3217/8. <https://eur-lex.europa.eu/legal-content/EN/TXT/PDF/?uri=CELEX:32013R1208&from=IT>.
- European Commission. (2013b). State of play in the EU on GM-free food labelling schemes and assessment of the need for possible harmonisation. In Publication Office of the European Union, European Commission Directorate General for Health and Food Safety https://ec.europa.eu/food/sites/food/files/plant/docs/gmo-traceability-gm-final_report_en.pdf.
- European Parliament and Council of the European Union. (2015). Directive (EU) 2015/412 of the European Parliament and of the Council of 11 March 2015 amending Directive 2001/18/EC as regards the possibility for the Member States to restrict or prohibit the cultivation of genetically modified organisms (GMOs) in their territory. *Official Journal of the European Union*, L68/1. <https://eur-lex.europa.eu/legal-content/EN/TXT/?uri=celex%3A32015L0412>.
- Franke, B. M., Haldimann, M., Baumer, B., Gremaud, G., Hadorn, R., & Kreuzer, J. B. M. (2007). Indications for the applicability of element signature analysis for the determination of the geographic origin of dried beef. *European Food Research and Technology*, 225, 501–509. <https://doi.org/10.1007/s00217-006-0446-2>
- García-Vaquero, M., Miranda, M., Benedito, J. L., Blanco-Penedo, I., & López-Alonso, M. (2011). Effect of type of muscle and cu supplementation on trace element concentrations in cattle meat. *Food and Chemical Toxicology*, 49(6), 1443–1449. <https://doi.org/10.1016/j.fct.2011.03.041>
- Ghidini, S., Varrà, M. O., Husáková, L., Alborali, G. L., Patočka, J., Ianieri, A., & Zanardi, E. (2022). Occurrence of toxic metals and metalloids in muscle and liver of Italian heavy pigs and potential health risk associated with dietary exposure. *Foods*, 11(16). <https://doi.org/10.3390/foods11162530>
- Halagarda, M., Kędzior, W., & Pyrzyńska, E. (2017). Nutritional value and potential chemical food safety hazards of selected traditional and conventional pork hams from Poland. *Journal of Food Quality*, 2017, 9037016. <https://doi.org/10.1155/2017/9037016>
- Halagarda, M., & Wójciak, K. M. (2022). Health and safety aspects of traditional European meat products. A review. *Meat Science*, 184, Article 108623. <https://doi.org/10.1016/j.meatsci.2021.108623>
- Heaton, K., Kelly, S. D., Hoogewerf, J., & Woolfe, M. (2008). Verifying the geographical origin of beef: The application of multi-element isotope and trace element analysis. *Food Chemistry*, 107(2081), 506–515. <https://doi.org/10.1016/j.foodchem.2007.08.010>
- Hrbek, V., Krtkova, V., Rubert, J., Chmelarova, H., Demnerova, K., Ovesna, J., & Hajšlova, J. (2017). Metabolomic strategies based on high-resolution mass spectrometry as a tool for recognition of GMO (MON 89788 variety) and non-GMO soybean: A critical assessment of two complementary methods. *Food Analytical Methods*, 10(11), 3723–3737. <https://doi.org/10.1007/s12161-017-0929-8>
- Italian Ministry of Agriculture, Food and Forestry. (2020). La competitività del settore suinicolo-Il quadro del settore, i trend emergenti e gli strumenti a supporto del rilancio della filiera nazionale. *Rete Rurale Nazionale 2014–2020*, 55. <https://www.terurale.it/flex/cm/pages/ServeBLOB.php/L/IT/IDPagina/22294>.
- Italian Ministry of Agriculture, Food Sovereignty and Forests. (2022). Amendment of the production disciplinary of the denomination «Prosciutto di Parma» registered as a protected denomination of origin pursuant to regulation (EC) n. 1107/96 of the Commission of 12 June 1996. (22A07334). *Official Gazette*, General Series n. 305 of 31-12-2022 https://www.gazzettaufficiale.it/atto/serie_generale/caricaDettaglioAtto/originario?atto.dataPubblicazioneGazzetta=2022-12-31&atto.codiceRedazione=22A07334&elenco30giorni=false.
- Italian National Institute of Statistics. (2023). 2022 slaughtering data - red meat monthly data. <http://dati.istat.it/Index.aspx?lang=en&SubSessionId=0b3de738-be2a-4d52-80c0-835c0f82f005>.
- Jerez-Timaure, N., Sanchez-Hildago, M., Pulido, R., & Mendoza, J. (2021). Effect of dietary brown seaweed (*Macrocystis pyrifera*) additive on meat quality and nutrient composition of fattening pigs. *Foods*, 10, 1720. <https://doi.org/10.3390/foods10081720>
- Jiang, J., Tang, X., Xue, Y., Lin, G., & Xiong, Y. L. (2017). Dietary linseed oil supplemented with organic selenium improved the fatty acid nutritional profile, muscular selenium deposition, water retention, and tenderness of fresh pork. *Meat Science*, 131, 99–106. <https://doi.org/10.1016/j.meatsci.2017.03.014>
- Kemper, N. P., Popp, J. S., Nayga, R. M., & Kerr, J. B. (2018). Cultural worldview and genetically modified food policy preferences. *Food Policy*, 80, 68–83. <https://doi.org/10.1016/j.foodpol.2018.09.003>
- Kim, J. S., Hwang, I. M., Lee, G. H., Park, Y. M., Choi, J. Y., Jamila, N., ... Kim, K. S. (2017). Geographical origin authentication of pork using multi-element and multivariate data analyses. *Meat Science*, 123, 13–20. <https://doi.org/10.1016/j.meatsci.2016.08.011>
- Lebret, B., & Čandek-Potokar, M. (2022). Pork quality attributes from farm to fork. Part II. Processed pork products. *Animal*, 16, Article 100383. <https://doi.org/10.1016/j.animal.2021.100383>
- Legislative Decree of the Italian Republic President 227/2016. (2016). Decreto Legislativo 14 novembre 2016, n. 227. Attuazione della direttiva (UE) 2015/412, che modifica la direttiva 2001/18/CE per quanto concerne la possibilità per gli Stati membri di limitare o vietare la coltivazione di organismi geneticamente modificati (OGM) sul loro territorio. *Gazzetta Ufficiale Della Repubblica Italiana*. https://www.gazzettaufficiale.it/atto/stampa/serie_generale/originario.
- Liu, X., Feng, X., Liu, F., Peng, J., & He, Y. (2019). Rapid identification of genetically modified maize using laser-induced breakdown spectroscopy. *Food and Bioprocess Technology*, 12(2), 347–357. <https://doi.org/10.1007/s11947-018-2216-0>
- López-Alonso, M., García-Vaquero, M., Benedito, J. L., Castillo, C., & Miranda, M. (2012). Trace mineral status and toxic metal accumulation in extensive and intensive pigs in NW Spain. *Livestock Science*, 146(1), 47–53. <https://doi.org/10.1016/j.livsci.2012.02.019>
- López-Alonso, M., Miranda, M., Castillo, C., Hernández, J., García-Vaquero, M., & Benedito, J. L. (2007). Toxic and essential metals in liver, kidney and muscle of pigs at slaughter in Galicia, north-west Spain. *Food Additives and Contaminants*, 24(9), 943–954. <https://doi.org/10.1080/02652030701216719>
- Meloun, M., Hill, M., Militký, J., & Kupka, K. (2000). Transformation in the PC-aided biochemical data analysis. *Clinical Chemistry and Laboratory Medicine*, 38(6), 553–559. <https://doi.org/10.1155/CCLM.2000.081>
- Miles, A. T., Hawksworth, G. M., Beattie, J. H., & Rodilla, V. (2000). Induction, regulation, degradation, and biological significance of mammalian metallothioneins. In *Vol. 35. Critical reviews in biochemistry and molecular biology* (pp. 35–70). CRC Press LLC. <https://doi.org/10.1080/10409230091169168>. Issue 1.
- Nikolic, D., Djinovic-Stojanovic, J., Jankovic, S., Stanic, N., Radovic, C., Pezo, L., & Lausevic, M. (2017). Mineral composition and toxic element levels of muscle, liver and kidney of intensive (Swedish Landrace) and extensive (Mangulica) pigs from Serbia. *Food Additives and Contaminants - Part A Chemistry, Analysis, Control, Exposure and Risk Assessment*, 34(6), 962–971. <https://doi.org/10.1080/19440049.2017.1310397>
- Oliveira, G. B., Alewijn, M., Boerrigter-Eenling, R., & van Ruth, S. M. (2015). Compositional signatures of conventional, free range, and organic pork meat using

- fingerprint techniques. *Foods*, 4(3), 359–375. <https://doi.org/10.3390/foods4030359>
- Parinet, J., Royer, E., Saint-Hilaire, M., Chafey, C., Noël, L., Minvielle, B., Dervilly-Pinel, G., Engel, E., & Guérin, T. (2018). Classification of trace elements in tissues from organic and conventional French pig production. *Meat Science*, 141, 28–35. <https://doi.org/10.1016/j.meatsci.2018.02.008>
- Park, Y. M., Lee, C. M., Hong, J. H., Jamila, N., Khan, N., Jung, J. H., ... Kim, K. S. (2018). Origin discrimination of defatted pork via trace elements profiling, stable isotope ratios analysis, and multivariate statistical techniques. *Meat Science*, 143, 93–103. <https://doi.org/10.1016/j.meatsci.2018.04.012>
- Qi, J., Li, Y., Zhang, C., Wang, C., Wang, J., Guo, W., & Wang, S. (2021). Geographic origin discrimination of pork from different Chinese regions using mineral elements analysis assisted by machine learning techniques. *Food Chemistry*, 337, Article 127779. <https://doi.org/10.1016/j.foodchem.2020.127779>
- Reig, M., Aristoy, M. C., & Toldrá, F. (2013). Variability in the contents of pork meat nutrients and how it may affect food composition databases. *Food Chemistry*, 140(3), 478–482. <https://doi.org/10.1016/j.foodchem.2012.11.085>
- Resano, H., Pérez-Cueto, F. J. A., Sanjuán, A. I., de Barcellos, M. D., Grunert, K. G., & Verbeke, W. (2011). Consumer satisfaction with dry-cured ham in five European countries. *Meat Science*, 87(4), 336–343. <https://doi.org/10.1016/j.meatsci.2010.11.008>
- Saleem, M. H., Ali, S., Hussain, S., Kamran, M., Chattha, M. S., Ahmad, S., ... Abdel-Daim, M. M. (2020). Flax (*Linum usitatissimum* L.): A potential candidate for phytoremediation? Biological and economical points of view. *Plants*, 9(4), 496. <https://doi.org/10.3390/plants9040496>
- Saraçlı, S., Doğan, N., & Doğan, İ. (2013). Comparison of hierarchical cluster analysis methods by cophenetic correlation. *Journal of Inequalities and Applications*, 213(1), 1–8. <https://doi.org/10.1186/1029-242X-2013-203>
- Sawosz, E., Kowalczyk, E., Hotowy, A., Lechowski, R., Kleczkowski, M., & Fabijanska, M. (2001). The effect of a diet fortified with polyunsaturated fatty acids on the level of selected elements in the myocardium of growing pigs. *Journal of Animal and Feed Sciences*, 10(2), 177–182. <https://doi.org/10.22358/jafs/70052/2001>
- Song, O. Y., Islam, M. A., Son, J. H., Jeong, J. Y., Kim, H. E., Yeon, L. S., ... Kim, K. S. (2021). Elemental composition of pork meat from conventional and animal welfare farms by inductively coupled plasma-optical emission spectrometry (ICP-OES) and ICP-mass spectrometry (ICP-MS) and their authentication via multivariate chemometric analysis. *Meat Science*, 172, Article 108344. <https://doi.org/10.1016/j.meatsci.2020.108344>
- Tomović, V. M., Sojić, B., Jokanović, M. R., Škaljac, S., Ivić, M., Tomović, M. S., ... Martinović, A. (2019). Mineral contents in pork and edible offal from indigenous pigs. *Journal of Engineering & Processing Management*, 11(1), 66–72. <https://doi.org/10.7251/JEPM1901066T>
- Tsagkaris, A. S., Koulis, G. A., Danezis, G. P., Martakos, I., Dasenaki, M., Georgiou, C. A., & Thomaidis, N. S. (2021). Honey authenticity: Analytical techniques, state of the art and challenges. *RSC Advances*, 11(19), 11273–11294. <https://doi.org/10.1039/d1ra00069a>
- Varrà, M. O., Husáková, L., Patočka, J., Ghidini, S., & Zanardi, E. (2021). Classification of transformed anchovy products based on the use of element patterns and decision trees to assess traceability and country of origin labelling. *Food Chemistry*, 360. <https://doi.org/10.1016/j.foodchem.2021.129790>
- Wójciak, K. M., Halagarda, M., Rohn, S., Keška, P., Latoch, A., & Stadnik, J. (2021). Selected nutrients determining the quality of different cuts of organic and conventional pork. *European Food Research and Technology*, 247(6), 1389–1400. <https://doi.org/10.1007/s00217-021-03716-y>
- Wold, S., & Sjöström, M. (1977). SIMCA: A method for analyzing chemical data in terms of similarity and analogy. In B. R. Kowalski (Ed.), *Chemometrics, theory and application* (pp. 243–282). s <https://doi.org/10.1021/bk-1977-0052.ch012>. s.
- Yang, W., Wang, K., & Zuo, W. (2012). Neighborhood component feature selection for high-dimensional data. *Journal of Computers*, 7(1), 161–168. <https://doi.org/10.4304/jcp.7.1.161-168>
- Zhao, L., Zhang, H., Huang, F., Liu, H., Wang, T., & Zhang, C. (2023). Authenticating Tibetan pork in China by tracing the species and geographical features based on stable isotopic and multi-elemental fingerprints. *Food Control*, 145, Article 109411. <https://doi.org/10.1016/j.foodcont.2022.109411>
- Zhao, Y., Tu, T., Tang, X., Zhao, S., Qie, M., Chen, A., & Yang, S. (2020). Authentication of organic pork and identification of geographical origins of pork in four regions of China by combined analysis of stable isotopes and multi-elements. *Meat Science*, 165, Article 108129. <https://doi.org/10.1016/j.meatsci.2020.108129>
- Zhao, Y., Wang, D., & Yang, S. (2016). Effect of organic and conventional rearing system on the mineral content of pork. *Meat Science*, 118, 103–107. <https://doi.org/10.1016/j.meatsci.2016.03.030>